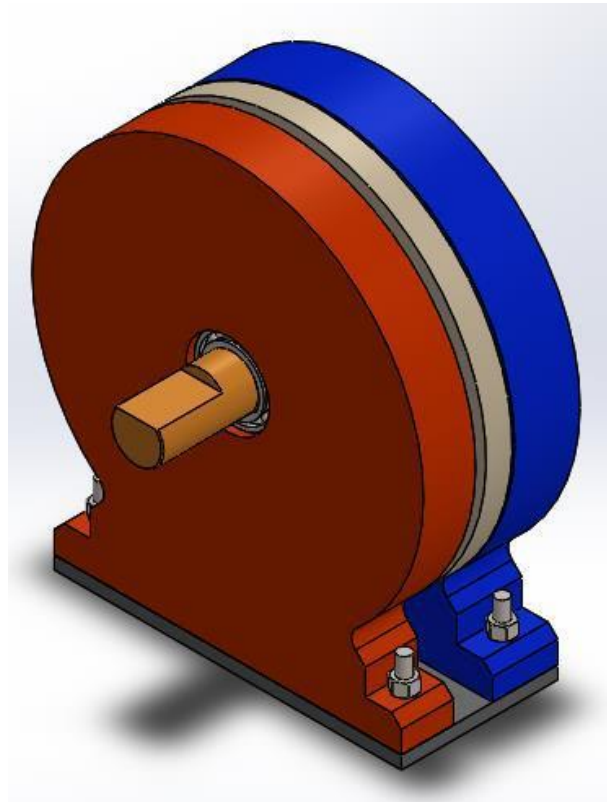




## AXIAL FLUX ELECTRIC MOTOR



*Juan Sebastián Lasprilla Hincapié*

*CC. 1016071495*

*Cel. 3183243634*

*Cód. 1802222*

*E-mail:*

*u1802222@uniMilitary .edu.co*

*Andresdavid Vargas Sandoval*

*CC. 1014268970*

*Cel. 3057106982*

*Cód. 1802394*

*E-mail:*

*u1802394@uniMilitary .edu.co*

*José Zuluaga Parra*

*CC. 1032465515*

*Cel. 3116055213*

*Cód. 1802491*

*E-mail:*

*u1802491@uniMilitary .edu.co*



## I. ABSTRACT

The goal for the research projects in electric motors is to help the adoption of new technologies that have greater engineering benefits and reduce environmental damage.

Taking as a base the innovation in axial flux electric motors, this project is conceived with the goal of achieving significant advances, in future stages of the project, in this application. The development presented in this article is still in progress and is susceptible to improvements.

## II. INTRODUCTION

The electric motor is a machine that transforms the electrical energy into mechanical energy, basing its principle of operation on the electromagnetic interactions of magnetic fields generated by the coils and magnets, housed in the structure [1]. Electrical machines are usually composed of one stator and one rotor.

Typically the electric motors are designed and constructed in order to use the radial flux distribution, where rotor and stator have a small radial air gap between them - Figure 1. In Axial flux motors, the winding can vary their geometric arrangement according to the required design diameter, making it possible to considerably reduce the total volume occupied by the machine.

The axial flux electric motors have specific positioning of their magnets, which are in planes parallel to the coils - Figure 2, which allows to create a flux of magnetic field over a smaller rotary volume resulting in a decrease of the moment of inertia and the mass of the rotor. [2]

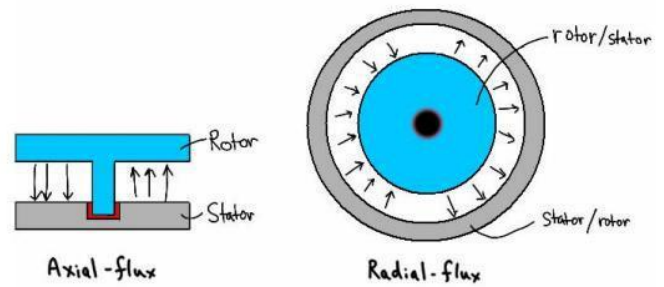


Figure 1. Rotor/Stator configuration in the radial and axial flux motor.

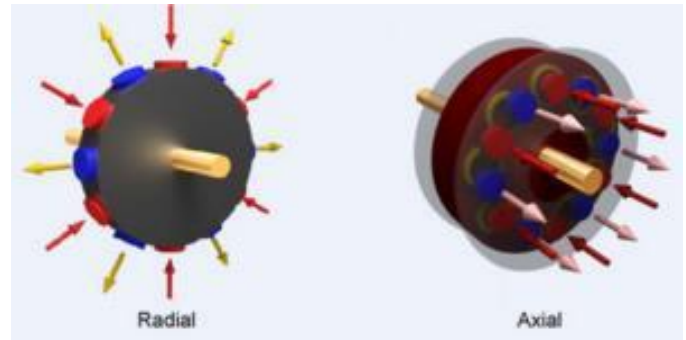


Figure 2. Radial VS axial PM Motor

The topic of this project is the design and manufacturing of an axial flux electric motor taking into account critical parameters such as size, electrical consumption and RPM. In order to conclude this project in the best way, all the development phases will be presented - from the working principle, through all the phases of analysis and design, both physical, electrical and electronic, to the control system.

## III. STATE OF THE ART

Basically, the electric motor is a machine that transforms electrical energy into mechanical energy by means of the action of the magnetic fields generated in its coils [3]. They are usually called rotating electrical machines and are composed of a stator and a rotor, some of which are reversible, and can function as motors or generators. On the other hand, electric traction motors

used in locomotives or hybrid cars often perform both tasks [3].

Historically axial flux machines were the first to develop- in 1821 Michael Faraday (British Physicist and Chemist) developed a primitive disk motor, which already had the shape of an axial flux machine, however, this machine had the disadvantage that it had a very large peak in the magnetization current due to the large air gap of the rotor disk, making it impossible to implement at that time [4].

Thanks to the advances made in the superconducting materials and permanent magnet materials, it has been possible to solve the problem that was had with the air gap, replacing it with conductive materials such as magnets of high remaining conduction such as the magnet of Neodymium (NdFeB) derived from the compound Nd<sub>2</sub>Fe<sub>14</sub>B discovered by General Motors (GM) in 1982 and by Sumitomo Special Metals in 1984, which developed dense synthesized magnets based on the discovered compound.

With the use of engineering materials developed specifically for use in electric motors, the use of electric machines could be imposed as a substitute for merely mechanical machines; Of which stand out the electrical machines of axial flux of permanent magnets (AFMPPM) or synchronous and the machines of induction (AFIM).

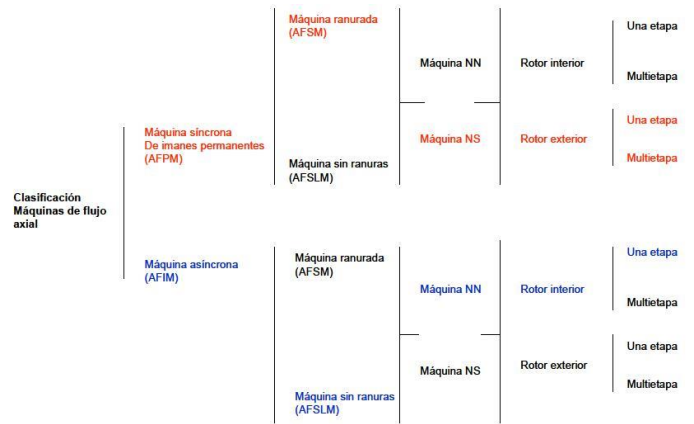


Figure 3. Classification of the axial flux machine.

- Axial Flux Motor with External PMs/ Axial Flux Motor with Internal PMs

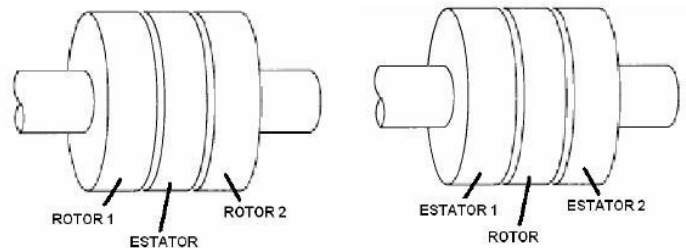
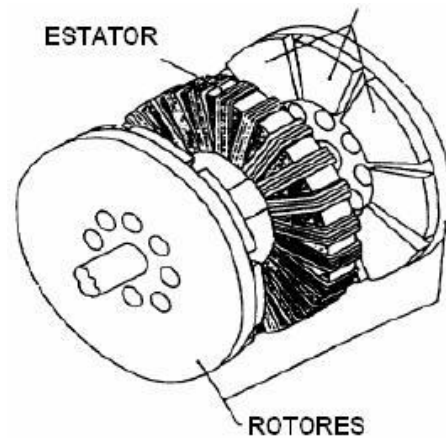


Figure 4. AFMIPM/AFMEPM

- Axial Flux Induction Motor



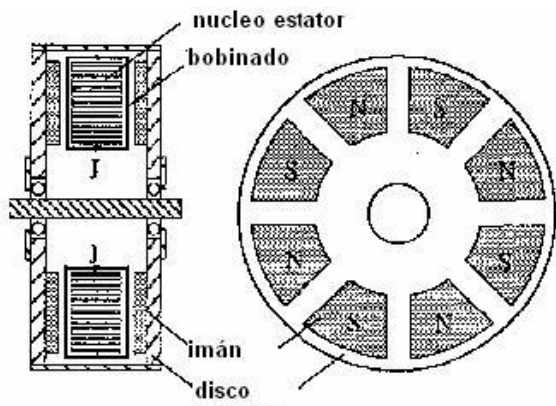


Figure 6. Axial flux machine with superconducting magnets.

- Double stator AF induction machine (type NN)

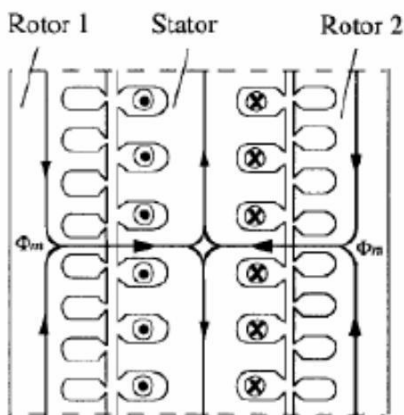


Figure 7. MFAIRNN

- Double stator AF induction machine (type NS)

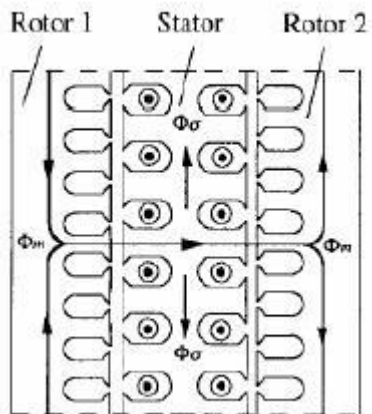


Figure 8. MFAIRNS

As shown, in the previous images, the structure of the axial flux motors is branched according to their type of construction Figure 3 [2].

As a principle of optimization and efficiency, the configuration of the axial flux motor represents a significant advantage with respect to the radial flux motor, for which this type of configuration is commonly used to ensure that the efficiency of the motor is greater than 90%. This way the company MAGNAX has developed Next-Gen Axial Flux Motor / Generator Figure 9 [5], which is a motor / generator of direct assembly that offers an efficiency of 96% for such specific purposes as wind turbines and electrical machinery of large industrial proportions, in addition to having a size of 140mm in length and 1600mm diameters, with a weight of 850kg, this engine / generator offers a torque of 16kNm.

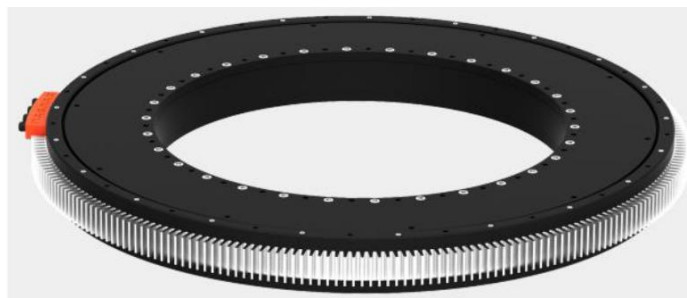


Figure 9. MAGNAX Next-Gen Motor/Generator

Permanent magnet axial flux motors allow the axial configuration to be maintained and the position of the rotating part to be changed to the ends of the motor, the **ELMO motor -S112** Figure 10 [6] of the company **ASHWOODS Electric Motor** has developed an engine of these characteristics maintaining a more compact design than that presented by the company **MAGNAX** in order to provide alternatives for smaller spaces. This engine delivers a torque of 45Nm at a speed of 5000 rpm, which allows to obtain an efficiency of 90%, the engine has a total weight of 13 kg.



Figure 10. AF Motor ELMO -S112.

Bearing in mind that this project is based on the construction of an axial flux electric motor, there are several ways to achieve electric control of these, one way that the electrical configuration of power is three-phase is to use the same principle used in the **EVO ELECTRIC** motor Figure 11 [7] of the company **CKN** which consists of 3 configurations of permanent magnets each fed with a phase, which increases the torque at the output due to the current density on the driven surface increases. This company has more than 5 models that allow you to choose between maximum speed (rpm), nominal torque (Nm), diameter (mm), length (mm) and weight (kg) as the most important options when choosing any of these Models.



Figure 11. EVO ELECTRIC

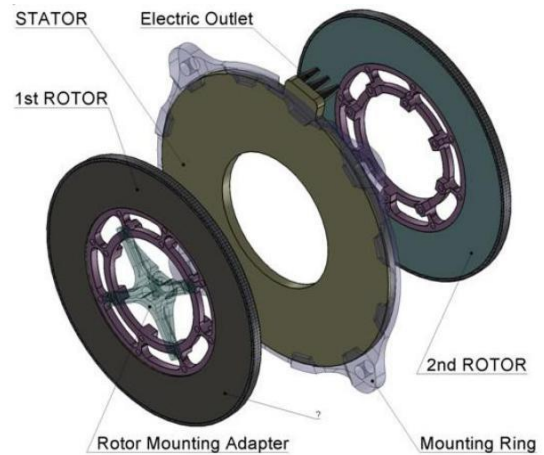


Figure 12. Brushless Coreless Axial-Flux Motors / Alternators

As seen in Figure 12 the company **ALBUS TECHNOLOGIES** [8] implements a double rotor motor making the ventilation on the stator is maximum, the innovation in the design presented by this company lies in the way they miniaturize each section of the same, allowing them to have a length between 2 and 5 mm with a maximum diameter between 8 and 15 mm, which facilitates its use in compact areas. With this design and its small size, this engine achieves a torque output between 5 and 8 Nm.

As we have seen so far, most of the designs presented handle the direct output of its axis parallel to the ground, which for many cases is useful, however, the company **LAUNCHPOINT TECHNOLOGIES, INC** [9] has managed to innovate in construction of the **HALBACH ARRAY ELECTRIC MOTOR** model, which is an axial flux electric motor with axis orientation perpendicular to the ground, as shown in Figure 13, which, in some cases, simplifies mechanical assembly because it does not need any type of coupling to change the direction of application of the torque.

This engine with its small design, less than 1 inch thick and approximately 6 inches in diameter, has a high structural strength that allows it to rotate at high revolutions (8400 rpm) generating approximately 7 horsepower per pound.

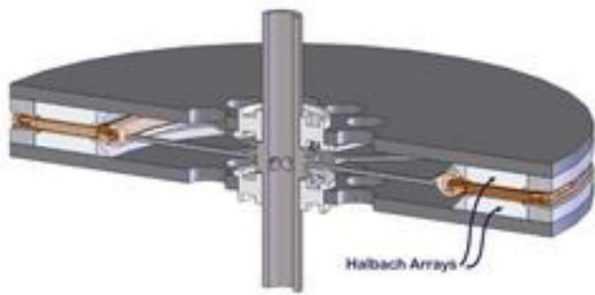


Figure 13. Halbach Array Electric Motor

Another example of the efficient use of space for electric motors with axial flux with three-phase power is the **EMRAX 188** motor Figure 14 - Figure 15 developed by the company **EMRAX INNOVATIVE E-MOTORS** [10], which changes the way of winding generating a greater rotor permeability generating in this way that the induced current density increases and a greater conduction and speed is generated as well. This engine with 188mm diameter and 77mm length delivers a torque of approximately 50Nm ensuring this 98% efficiency.



Figure 14. EMRAX 188

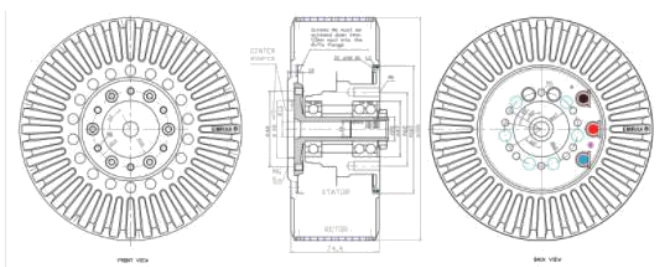


Figure 15. EMRAX 188 Cross-section

As a last example, we present the brushless axial flux DC motor with air core coils, developed by the company **DUNKENMOTOREN and AMETEK Advanced Motion Solutions**, which directly implies that there is no induced field that generates any type of vibration, this in mechanical design allows its efficiency to be greater than in other previously presented designs. The principle of operation is the same, however, this has greater induced current density, which allows it to maintain a greater robustness in terms of its electromagnetic composition.



Figure 16. Brushless DC Motor BGA 22x2 d Core

#### IV. THEORETICAL BACKGROUND

Within the category of electric motors we can find two configurations; Radial flux motor (MFR) is characterized when the resulting magnetic field rotates like the hands of a clock, superimposed perpendicularly along the axis, and axial flux motor (MFA) which is characterized when the magnetic field resulting from a Certain motor rotates concentric to its axis, besides that these present high values of motor torque at low speeds, high efficiency and high power density - Figure 17 - Figure 18 - Figure 19 - Figure 20 [2].

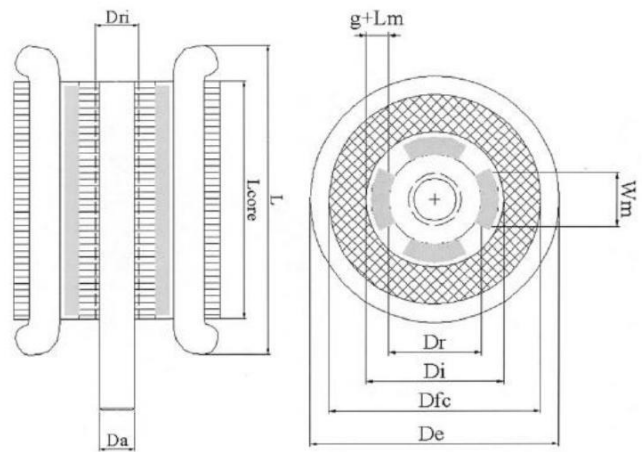


Figure 17. Important dimensions of a AF motor

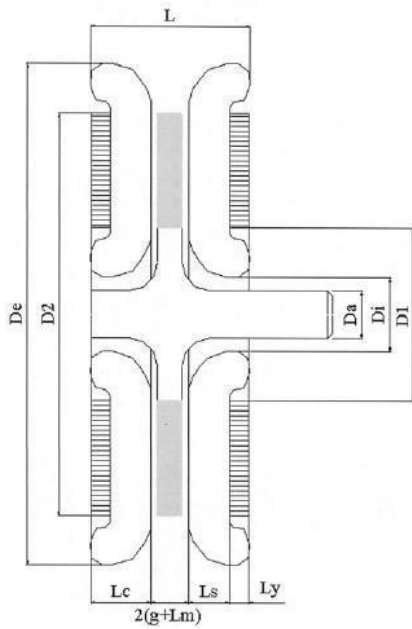


Figure 18. Important dimensions of a AF motor.

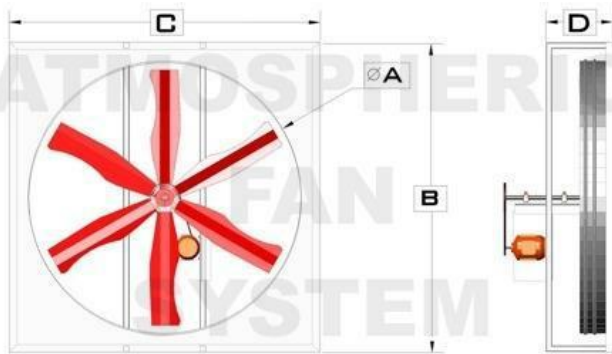


Figure 19. Normal distribution of an AF Motor

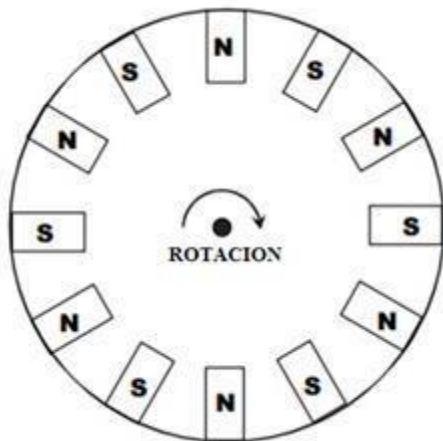


Figure 20. Permanent magnet distribution

The operation of an axial flux motor is based on the interaction of the magnets in the rotor with the electromagnetic field flux produced by the coils, generating an induction of current on the rotor to generate a rotational torque, the explanation of this phenomenon

Physical is based on the Lorentz Force, which dictates that "Any electric charge moving within a magnetic field suffers a force" [12].

$$\vec{F} = q(\vec{v} \times \vec{B})$$

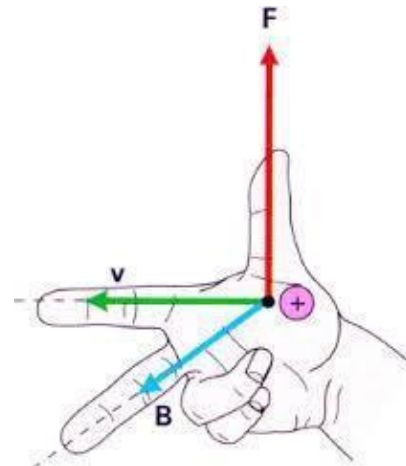


Figure 21. Graphical representation of the Lorentz Force.

With this principle is that the movement of the electric motor is achieved since maintaining constant the polarity of the load and varying the direction of flux of the magnetic field can generate the movement, due to the force rotations, for or against the hands of the clock.

Figure 22 and Figure 23 show the two cases that can be presented according to the direction of the movement that is generated, in this case the direction of the current on the winding Figure 30. The change of direction of the current must be generated in order to attracting the poles of the magnets distributed according to Figure 20 so as to generate attraction and repulsion forces on each section of magnets.

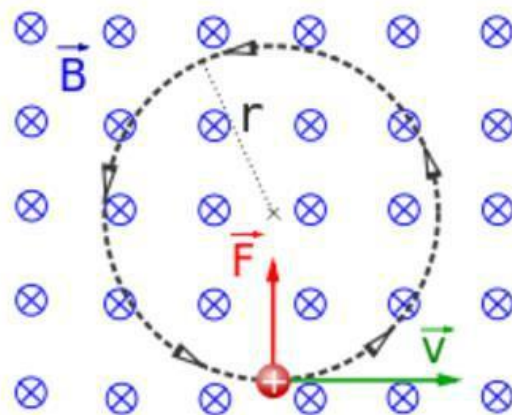


Figure 22. Rotational Lorentz force with a positive charge

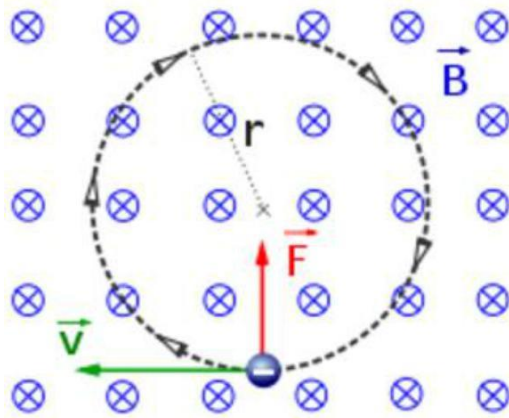


Figure 23 Rotational Lorentz force with a positive charge

The advisable way to make all the changes in the direction of the magnetic fields can be described according to the shape of the wave in Figure 24, in which during half a cycle the wave maintains positive values of current that generate a positive magnetic change and in its other half cycle it takes negative values that invert the sense of the magnetic field, in general it could be said that the available three-phase power of the public network can be used but the main problem with this power supply is that the frequency that is handled, 60 Hz, for basic applications it is difficult to control, for which reason another means of feeding must be available.

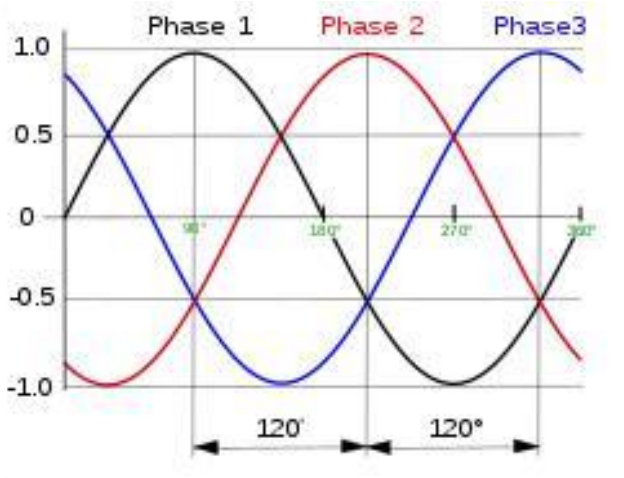


Figure 24. Three-phase waveform of the public power network.

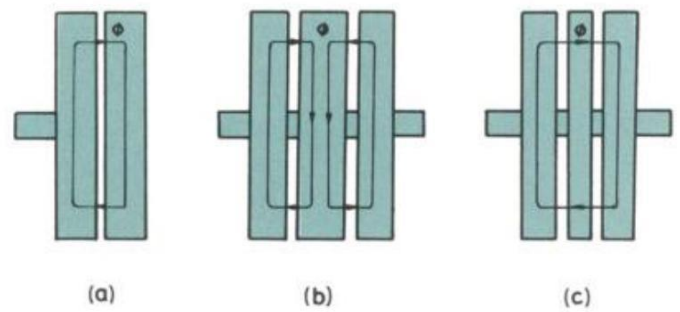


Figure 25. Possible configurations for axial flux motors.

In order to simplify the prototype model developed in this project, it was proposed to use the configuration (a), shown in [2], facilitating the development of the electronic part since it is not necessary to have control over both rotors to synchronize the stages with the sending of the necessary sequences for the movement of the motor, nor to develop more electrical power if the configuration of double stator is handled.

Taking into account both the physical and electromagnetic aspects of the system, emphasis is placed on the following parameters;

- Magnitude of the electromagnetic
- Induced magnetization force
- Stator dimensions for coil design
- Geometrical structure of the winding to maximize the induced field
- Resistivity, inductance, reluctance and impedance of the windings

In order to have these parameters as a basis, it is necessary to know how the principles of magnetization work on a solenoid and for this the following information is exposed;

The composition of the coils can be modeled as an N-turn solenoid, forming a configuration of length L, distributed one after the other with one or several layers as shown in Figure 26.

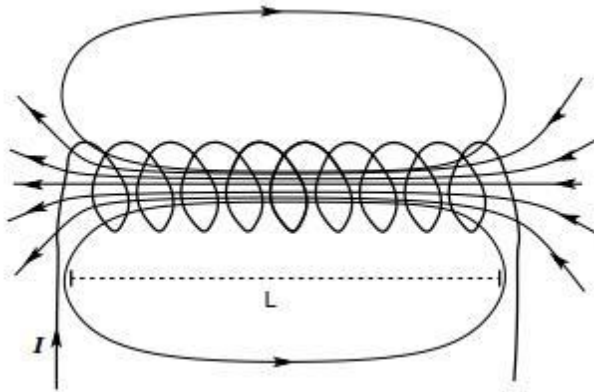


Figure 26. Simplified flux distribution of a solenoid.

Taking into account that the coils are going to be solenoids, with a defined shape, the magnetic field on these can be described in [13] as

$$B = \frac{\mu N I}{l}$$

Equation 2. Magnetic field equation of a solenoid, where:

- $\mu$ , magnetic vacuum permeability coefficient, being equal to  $4 \cdot 10^{-7} / 2$  if no nucleus is used.
- N, total number of turns in the solenoid.
- I, magnitude of the current fluxing in the solenoid.
- l, total winding length.

Once the magnetic field generated by the coil supply in one direction is known, the magnitude of the dipole magnetic moment on each loop can be known in the following way described in [13] as:

$$\tau_e = IBA \sin \phi$$

Equation 3. Magnetic dipole moment equation in a solenoid loop.

- Where;
- B, magnetic field present in the solenoid.
- I, magnitude of the current fluxing in the solenoid.
- A, induction area of the magnetic field.
- $\phi$ , angle of incidence of the magnetic field with respect to the perpendicular of the plane of the turn.

Knowing that the solenoid is composed of N contiguous spiers, we can determine that the magnitude of the total torque on the solenoid is the sum of each of the moments generated by each turn, therefore, the dipole moment on a solenoid is:

$$\tau = NIBA \sin \phi$$

Equation 4. Magnetic dipole moment equation in one loop of the solenoid, where:

- B, magnetic field present in the solenoid.
- I, magnitude of the current fluxing in the solenoid.
- A, induction area of the magnetic field.
- $\phi$ , angle of incidence of the magnetic field with respect to the perpendicular of the plane of the turn.
- N, total number of turns in the solenoid.

In this way it is possible to quantify the magnitude of both the force and the attraction as well as the repulsion which are necessary for the movement of an electric axial flux motor to be generated.

In conclusion, the phenomenon that occurs for the existence of electromagnetic induction motors is that both the winding field Figure 26, generally solenoids, and the field generated by the permanent magnet attempt to align so that their magnetic fields form a single loop. Repeating this process again and again, changing the direction of the magnetic field induced in the coil, generate the forces of attraction and repulsion that manifest the movement of the rotors in the motors.

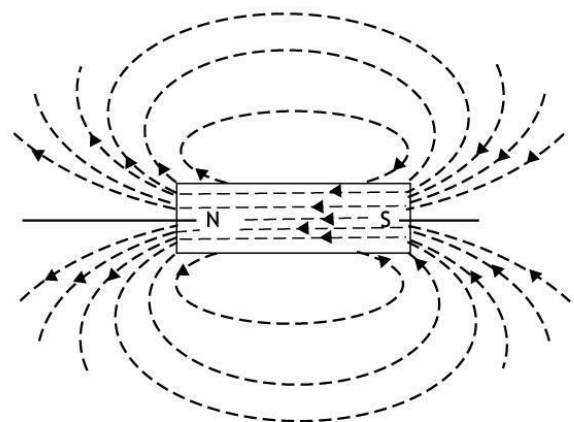


Figure 27. Magnetic field lines of a magnet.

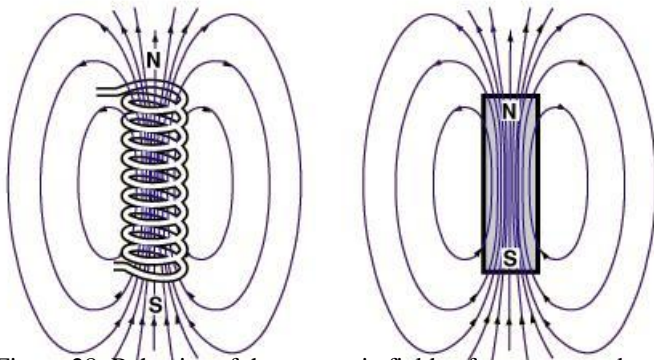


Figure 28. Behavior of the magnetic fields of a magnet and a solenoid.

Having clear the phenomena that make feasible the operation of the proposed project is presented in Figure 29 the shape of the coils that are going to be implemented in the assembly. This geometric configuration was chosen in order to distribute the magnetic field in a directed manner over each magnetic field of the magnets resulting in the reduction of the electromotive force that must be generated to attract each pair of magnets. The selection of this type of geometric shape for the coils was made on the study proposed in [2] by Miguel Juan Pallarés Viña, where a three-phase double-layer winding is used, implementing one slot per pole and phase. The structure of the winding is made in a malt cross configuration with the intention of generating a wave of sinusoidal magneto-motive force [2].

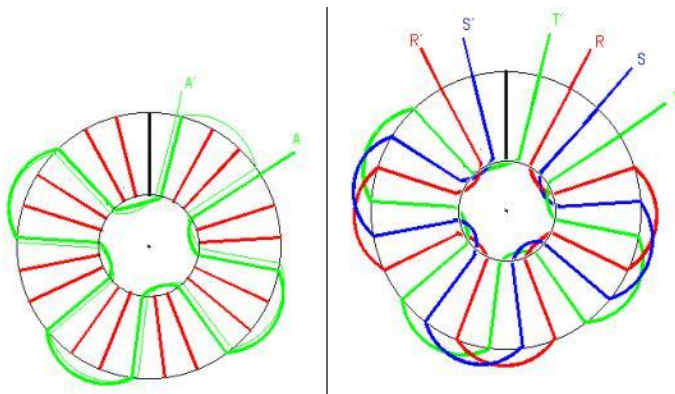


Figure 29. Malt cross shape for winding.

Projecting an expected speed that has our axial flux electric motor, we apply Equation 5 that correlates the frequency with the number of poles to estimate the maximum revolutions that can reach our system.

$$rpm = \frac{120 f}{\# \text{ polos}} = \frac{120 (60)}{8} \cong 900$$

Equation 5. Maximum revolutions

where:

- f, magnetic circuit inductance
- f, working frequency
- R, resistance of the electrical circuit.

## V. Design

### 1. STRUCTURE OF THE PROJECT

The purpose of this project is to make an electric motor of axial flux that is capable of rotating at a speed of 100 rpm for or against the clockwise, besides that it is possible to vary its speed, to achieve this end All the calculations for design proposed in **Numeral IV** of this article are implemented.

The structure of the engine will be made in acrylic, this material was chosen because it has a very high modulus of elasticity with respect to the forces that will be generated in the structure, according to [14] under the method ASTM D-638 the PC compact polycarbonate its value is in the range of 600 to 680 kg / cm<sup>2</sup>.

The remaining materials described in Table 1 were selected according to our needs from the catalogs SKF [15], Screws and Nuts [16], Magnets [17] and AWG [18].

Propiedades mecánicas	Unidades	Normas Astm	ACRILICO PAQUETE Colado	Acrílico Extruido	Ignifugo	Extruido Alto Impacto
<b>Tracción</b>						
Resistencia en el límite elástico	Kg/cm <sup>2</sup>	D-638	-	-	-	-
Resistencia a la rotura	Kg/cm <sup>2</sup>	D-638	562-773	492-773	562-878	386
Elongación a la rotura	%	D-638	4,5	5,0	5,0	-
Módulo de la elasticidad	Kg/cm <sup>2</sup>	D-638	24.600-31.000	23.000-31.000	26.600-33.700	-
<b>Flexión</b>						
Resistencia en el límite elástico o rotura	Kg/cm <sup>2</sup>	D-790	840-1.190	740-1.300	840-1.250	562
Módulo de elasticidad	Kg/cm <sup>2</sup>	D-790	27.500-33.400	22.800-32.300	24.600-31.600	17.500
<b>Compresión</b>						
Resistencia a la compresión (ruptura)	Kg/cm <sup>2</sup>	D-695	773-1.330	740-1260	773-840	-
Módulo de compresión	Kg/cm <sup>2</sup>	D-695	27.500-33.300	26.000-32.300	31.000	-
<b>Impacto</b>						
Resistencia al impacto IZOD	Kg/cm/cm	D-256 A	1,9	2,4	1,9	6,52
<b>Dureza Rockwell Barcol</b>						
Dureza Rockwell		D-795	M-80- M-100	M-68- M105	M-61- M-100	R-99
Dureza Barcol		D-2583	50	50	45	35
<b>Propiedades Térmicas</b>						
Coefficiente de dilatación lineal	cm/cm°C	D-696	6,0 x 10 <sup>-6</sup>	1,3 x 10 <sup>-6</sup>	1,3 x 10 <sup>-6</sup>	-
Temperatura de deflexión bajo carga	18% kg/cm	D-648	86°C	74-99°C	68-96°C	82°C
Conductividad térmica	10 <sup>-4</sup> cal cm/sec cm <sup>2</sup> °C	C-177	4,0-6,0	4,0-6,0	4,0-6,0	-
Calor específico	Cal/g°C		0,35	0,35	0,35	0,35
<b>Propiedades físicas</b>						
Peso específico	g/cm <sup>3</sup>	D-792	1,191,20	1,19,120	1,23	1,15
Absorción de agua	%	D-570	0,2-0,4	0,1-0,4	0,63	0,4
<b>Propiedades eléctricas</b>						
Resistencia eléctrica	Ohm/cm	D-257	>10 <sup>8</sup>	>10 <sup>8</sup>	>10 <sup>8</sup>	-
Rigidez dieléctrica	Kv/mm	D-149	19	17	16	-

Figure 30. Polymer properties of Acrylic

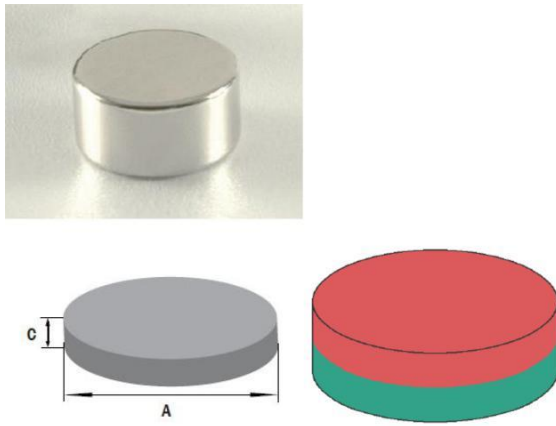


Figure 31. Dimensions and magnetization of the neodymium magnet

AWG	DIAMETRO (inch)	DIAMETRO (mm)	RESISTENCIA (Ohms/Km)	RESISTENCIA (Ohms/Ft)	AMPERAJE A 60°/75°/90°
8	0,1285	3,264	2,061	0,6282	40/50/55
10	0,1019	2,588	3,277	0,9989	30/35/40
12	0,0808	2,053	5,211	1,588	25/25/30
14	0,0641	1,628	8,286	2,525	20/20/25
16	0,0508	1,291	13,17	4,016	18
18	0,0403	1,024	20,95	6,385	14
20	0,032	0,812	33,31	10,15	-
22	0,0253	0,644	52,96	16,14	-
24	0,0201	0,511	84,22	25,67	-

Figure 32 AWG table for wire gauge.

Likewise, a quality house structure is proposed to take into account possible benefits expected by a possible user or ourselves as designers of the project. And also the embedded device that will facilitate the control stage of the project Figure 34.

Requerimientos del cliente	Características de Ingeniería	Importancia para el cliente (1-5)	Consumo de energía								Tipo de Arranque			
			Material	Alto	Largo	Ancho	Apariencia	Velocidad	Torque	Disipación de energía	Independencia Energética	Partes Fusibles		
1	Fácil de transportar	3	1	3	9	9	9	1	1	1	1	3	3	1
2	Manejo de torques	2	9	9	3	3	3	1	3	9	3	3	9	3
3	Manejo de altas velocidades angulares	2	9	9	1	1	1	1	9	3	3	3	9	3
4	Liviano	2	1	9	3	3	3	1	1	3	3	1	3	1
5	Fácil mantenimiento	4	1	1	3	3	3	1	3	3	9	1	9	9
6	Desarmable	5	1	9	3	3	3	1	1	1	9	3	9	9
7	Eje extendido	4	3	9	3	3	3	1	3	3	1	1	1	3
8	A prueba de agua	4	1	9	1	1	1	3	1	1	9	9	3	9
9	Inoxidable	5	1	9	1	1	1	3	1	1	3	9	3	9
10	Tamaño	4	3	1	1	1	1	1	3	3	9	9	9	1
11	Presentación	1	3	1	1	1	1	9	1	1	1	3	1	1
EVALUACIÓN TÉCNICA	ABSOLUTA	83	233	93	93	93	53	79	83	193	163	199	195	
	RELATIVA (%)	6	15	6	6	6	3	5	5	12	10	13	13	

Figure 33. Project matrix QFD.

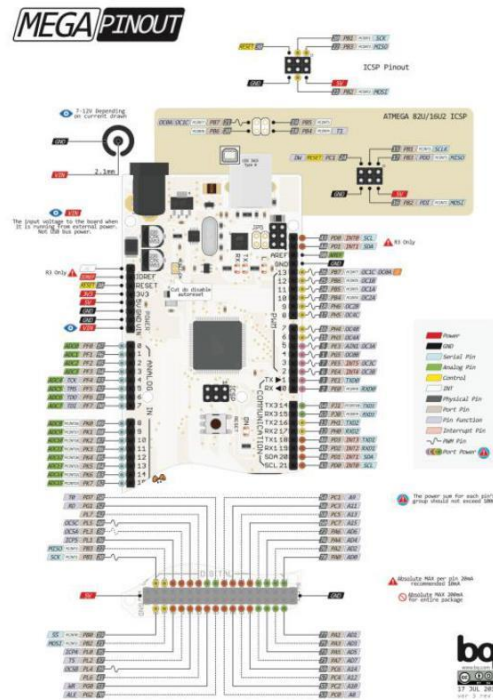


Figure 34. Schematic of input / output pins of the Arduino Mega 2560.

## 2. DESIGN SPECIFICATIONS

The following are the main requirements for the system:

- The power must be by external DC source.
- The minimum speed must be 100 rpm.
- It must be possible to vary the speed of the system.
- It must be possible to change the direction of rotation.

Additionally, the use of an axial flux electric motor is recommended when these parameters are required:

- Low speeds.
- Elevated pairs.
- Machine weights necessarily low.
- High and frequent overloads.

□ **INITIAL PROJECT DESIGN PROCESS**

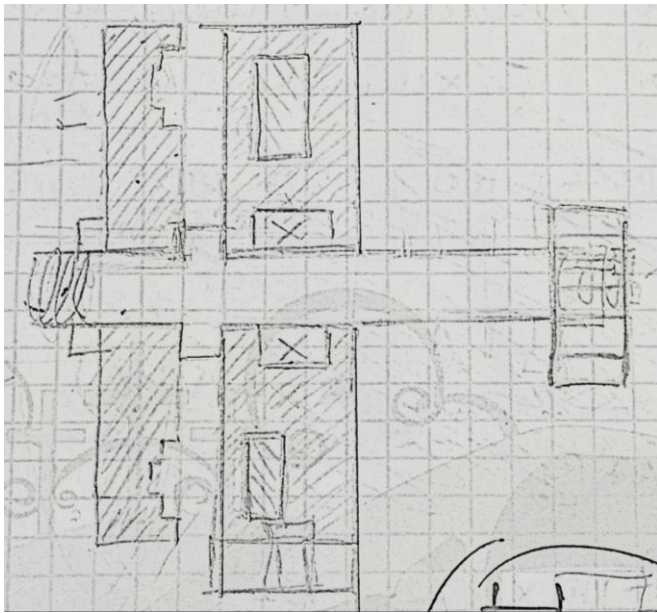


Figure 35. Initial sketch of the motor structure.

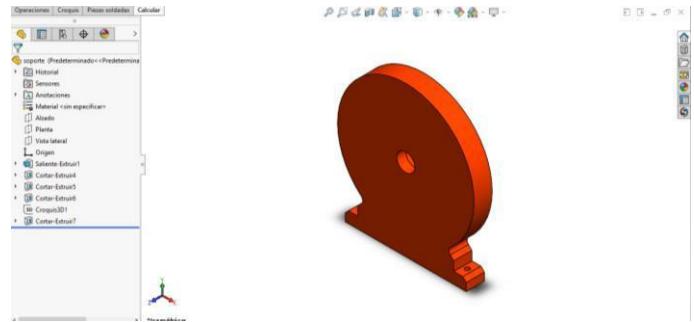


Figure 38. Final design engine support.

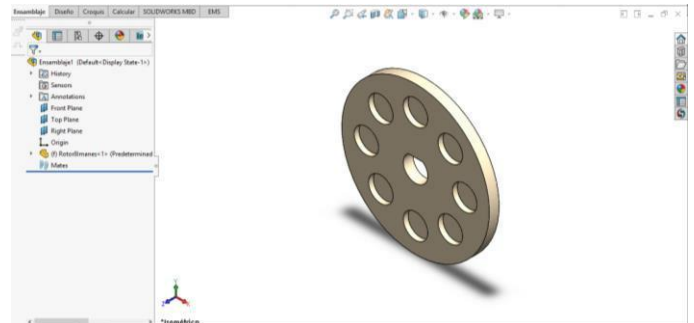


Figure 39. Rotor design.

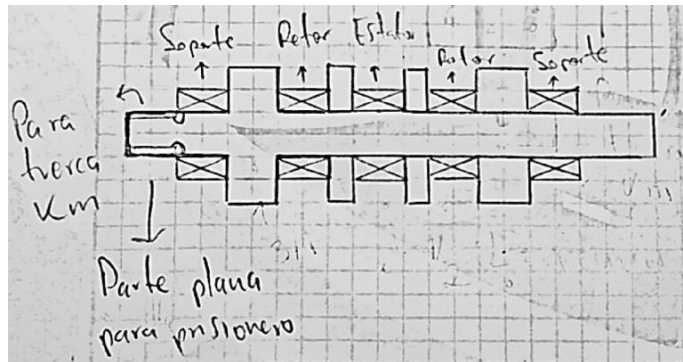


Figure 36 Sketch of the motor shaft.

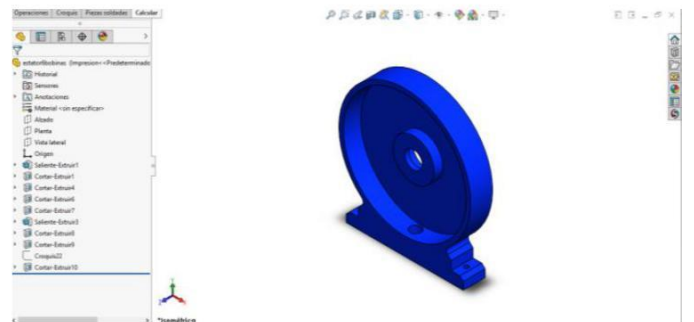


Figure 40. Stator support design.

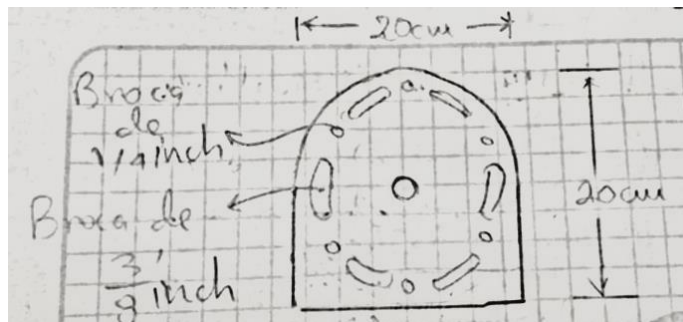


Figure 37. Sketch of the motorcycle support structure.

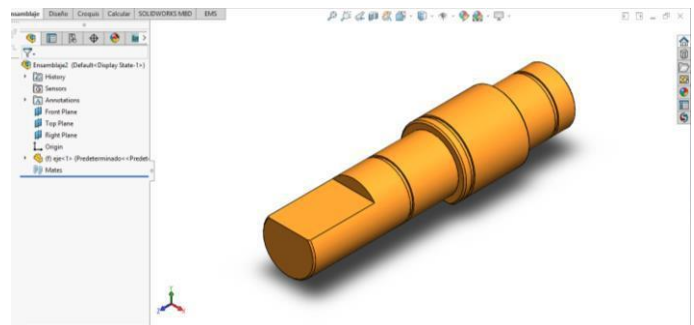


Figure 41. Final design of the motor shaft.

□ **FINAL PROJECT DESIGN PROCESS**

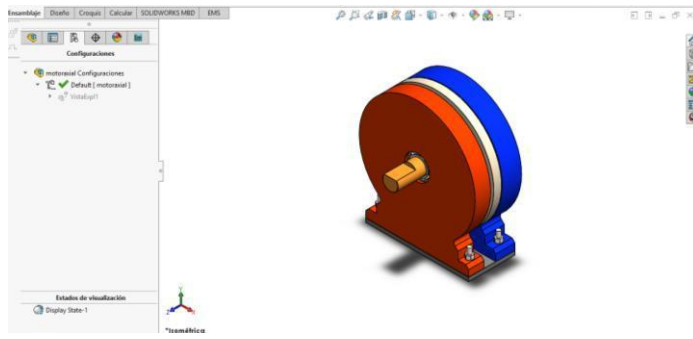


Figure 42. Final assembly of the motor model.

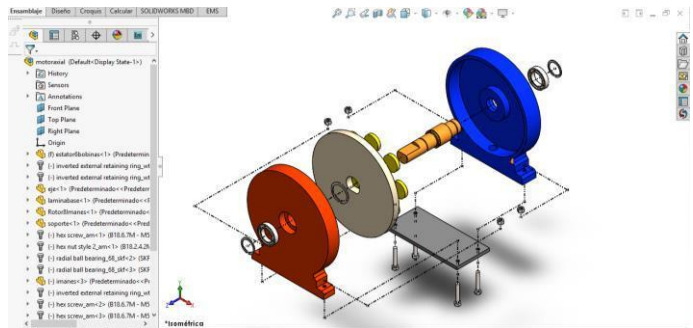


Figure 43. Total motor assembly.

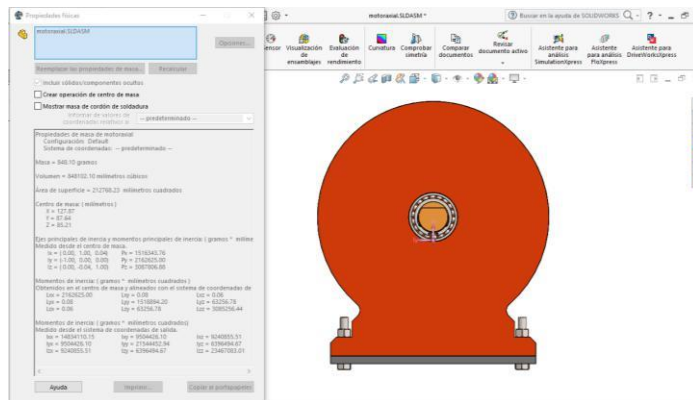


Figure 44. Properties, center of mass of the final assembly of the model.

**5. BUDGET AND COSTS**

In order to publicize the project is fully in Table 1 all the expenses incurred for the mechanical, electronic and electrical part are presented.

Material/Part	Qty.	Cost	Total Cost
Package 1inx50cm	1	\$ 4.900	\$ 4.900
mechanical services	-	\$ 30.000	\$ 30.000
Neodymium Magnet	10	\$ 3.200	\$ 32.000

Twin Resins 500ml	1	\$ 22.000	\$ 22.000
Screw M5x30	20	\$ 500	\$ 10.000
Nut M5	20	\$ 500	\$ 10.000
Tread SKF	2	\$ 5.000	\$ 10.000
Retaining Rings DSI	2	\$ 4.450	\$ 8.900
Acrylic 5mm	3	\$ 70.000	\$ 70.000
Cutting Acrylic	-	\$ 30.000	\$ 30.000
Enameled Wire Copper (g)	1200	\$ 47.000	\$ 47.000
Lamination MDF 5mm	1	\$ 8.000	\$ 8.000
Lamination MDF 3mm	1	\$ 5.000	\$ 5.000
Service Corte Laser MDF	-	\$ 10.000	\$ 10.000
Capacitor 10 mF	6	\$ 100	\$ 600
Resistencia 10W 10 ohm	9	\$ 600	\$ 5.400
Resistencia 1/4W 10 K ohm	10	\$ 20	\$ 200
MOSFET IRF 540	12	\$ 2.500	\$ 30.000
Transistor 2n2222 NPN	12	\$ 100	\$ 1.200
Transistor 2n3906 PNP	6	\$ 100	\$ 600
Diode 1n5408	6	\$ 250	\$ 1.500
Arduino Mega 2560	1	\$ 40.000	\$ 40.000
Estimated time man-hours (3 engineers)	100	\$ 25.000	\$ 2.500.000
<b>TOTAL (without Estimated time)</b>			\$ 337.300
<b>TOTAL (with Estimated time)</b>			\$ 2.872.400

Table 1. Budget and Costs

**6.1 PERMANENT MAGNET SIMULATION**

In order to support the design process, a simulation was used to study the actual behavior of the magnets, before the project was initiated.

EMS by EMWorks is an electromagnetic simulation software that has been donated to us by EMWorks for this project. Thanks to EMS, the simulation of the real-life permanent magnet behavior could be implemented. To start the simulation, it is necessary to first create a 3D model - Figure 45 - of the permanent magnet. The material assigned to the model is Neodymium N4212.

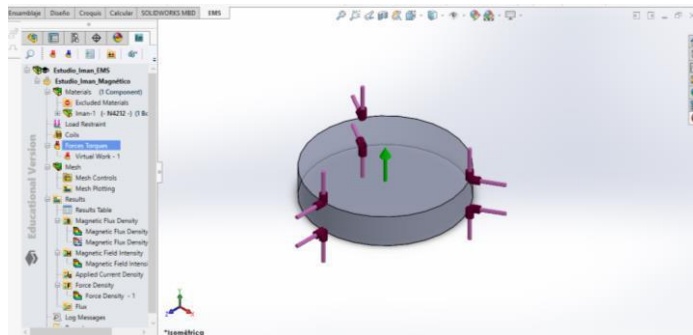


Figure 45 Model for simulation of a neodymium magnet.

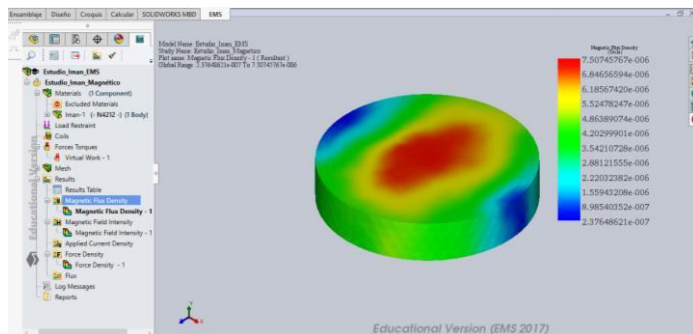


Figure 46. Magnetic Flux Density fringe plot (Tesla)

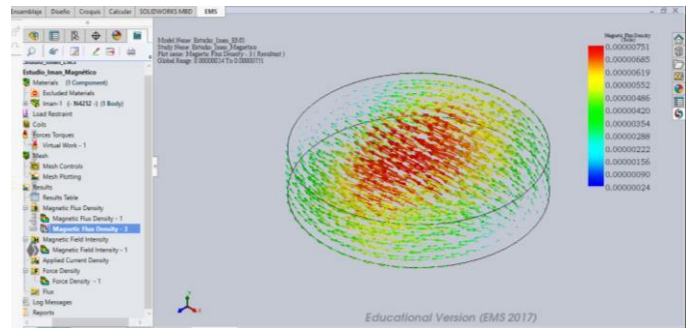


Figure 47 Magnetic Flux Density Vector plot (Tesla)

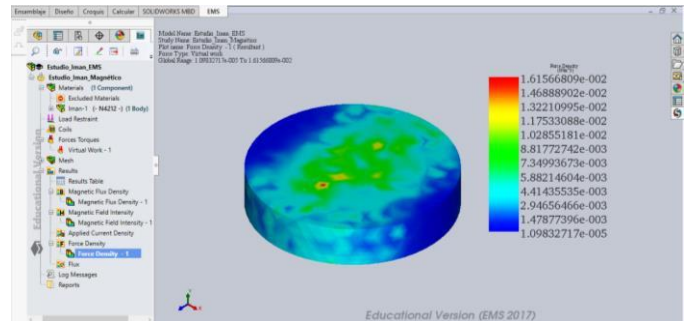


Figure 48. Force density graph (N/m<sup>3</sup>).

Some of the simulation results include: Magnetic flux density in Figure 46, Magnetic field lines in Figure 47 and Magnetic Force density in Figure 48. This has been done in order to verify that permanent magnets will be attracted by the magnetic fields generated by the coils.

**6.2 PROPOSED SIMULATION ANALYSIS FOR THE ROTOR**

Below are the simulation results for the magnets inserted in the rotor. This simulation analysis provided a visual support for how the fields of the magnets interact when they are arranged in a circular pattern alternately exchanging the pole orientation. Fiberglass, a material with low magnetic permeability, has been assigned to the rotor.

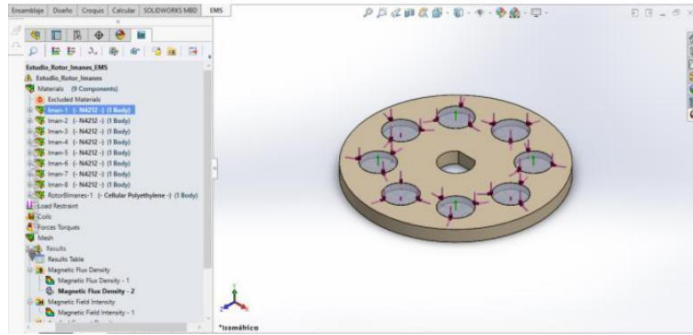


Figure 49. Model for simulation of the rotor with neodymium magnets.

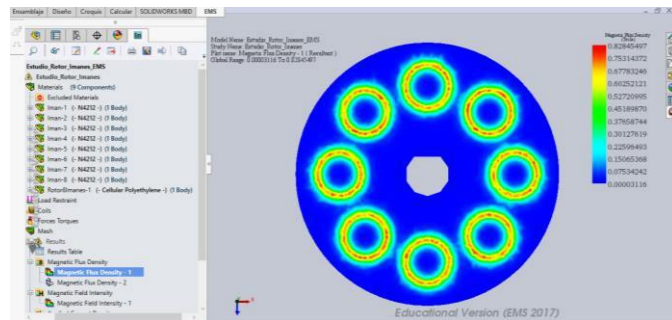


Figure 50. Magnetic Flux Density (Tesla)

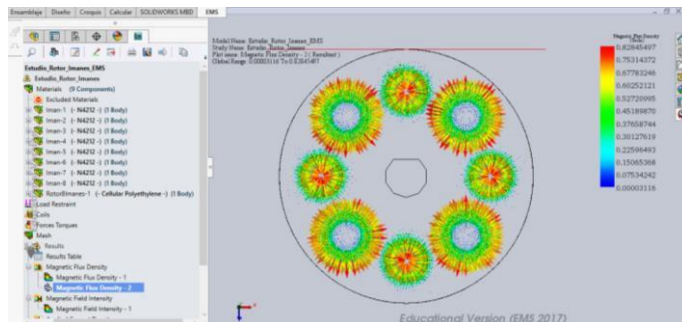


Figure 51. Magnetic Flux Density Lines (Tesla)

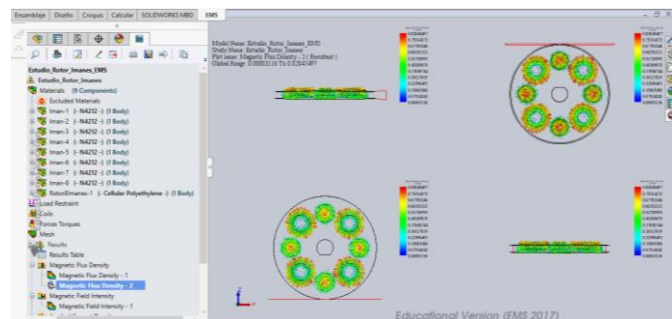


Figure 52. Magnetic Flux Density Lines for both sets of magnets (Tesla).

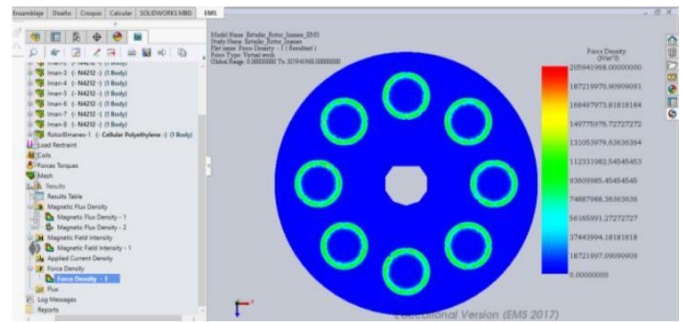


Figure 53. Force density graph (N/m<sup>3</sup>).

### 6.3 PROPOSED SIMULATION ANALYSIS FOR THE COIL

The simulation of the coil was carried out in order to verify by means of a specialized software, in this case EMS for SolidWorks, that the magnetic field is in the ranges of magnitude necessary to meet the specifications for the proper functioning of the project.

As a first step to perform the simulation of the coil in EMS software, a 3D model of the coil is required, which is shown in Figure 54.

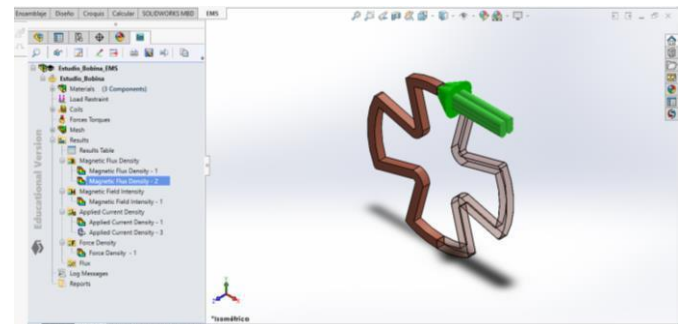


Figure 54. Coil model in SolidWorks.

On this model it is necessary to indicate the cross-section area by which the current enters the coil; for this reason the coil model is split is half (Figure 45).

As a next step in the simulation it is necessary to define materials for the models; it is indicated that for this study the coil is made of 18-gauge enameled copper wire.

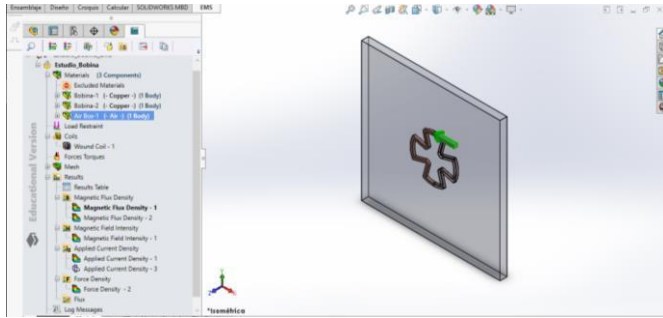


Figure 55. Air core for coil simulation.

Coil definition is finalized by entering the number of turns, wire gauge and the magnitude of the current excitation, as in Figure 56.

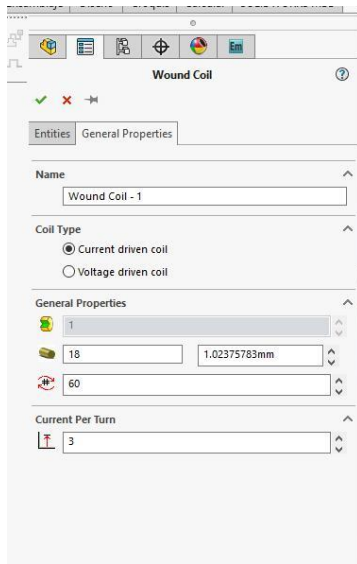


Figure 56. Defining the coil in EMS.

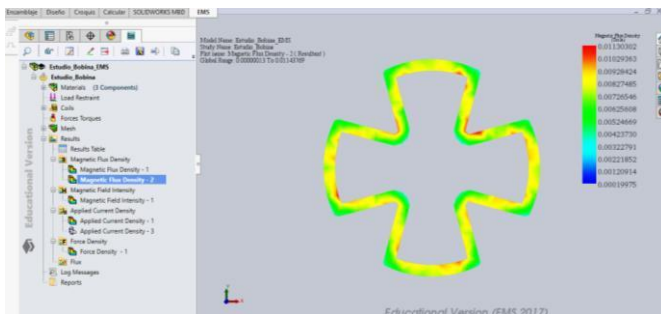


Figure 57. Coil Flux density (Tesla).

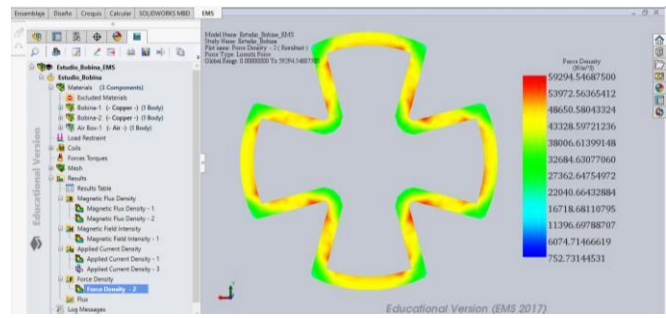


Figure 58. Force density in the coil.

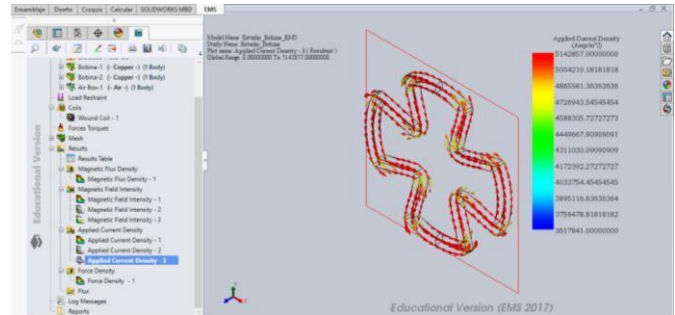


Figure 59. Current density in the coil.

The results of the magnetic flux density are presented in Figure 57, magnetic force density in Figure 58 and the density of the applied current in Figure 59. If the magnetic field or current intensity were not sufficient, it would be necessary to redesign the coils and ensure that these values would match the conditions set by the project.

#### 6.4 SIMULATION ANALYSIS OF THE THREE-PHASE INVERTER

Based on the previous explanation of the operation of the three-phase inverter, it is shown that the previously made analysis agrees with the voltage forms at the output of the three-phase inverter circuit, taking into account that the inputs of the pulses for the control of the three-phase inverter are shown in Figure 75, it is verified that the line-neutral voltages shown in Figure 71 simulated and tested in real life, agree with the approximate theoretical results shown in Figure 62. As well as the line-line voltages taken at the circuit output. The real values shown in Figure 76 are consistent with the theoretical result shown in Figure 62.

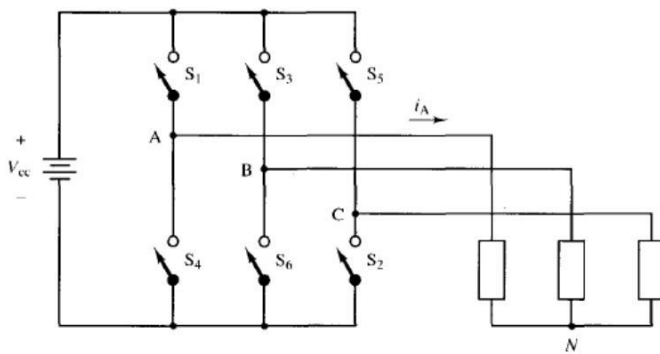


Figure 60. Three-phase alternating current circuit from a DC input.

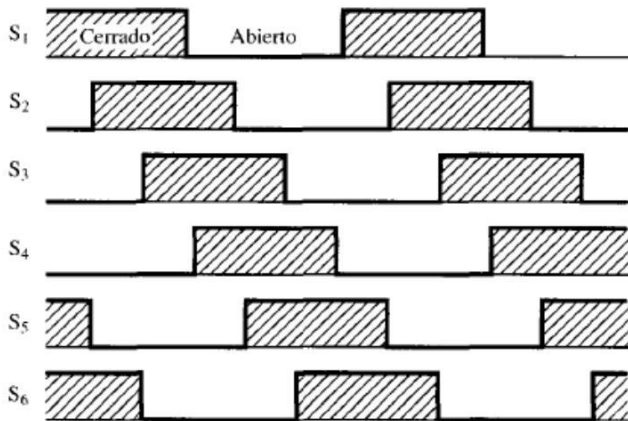


Figure 61. State diagram of the switches shown in Fig. 60

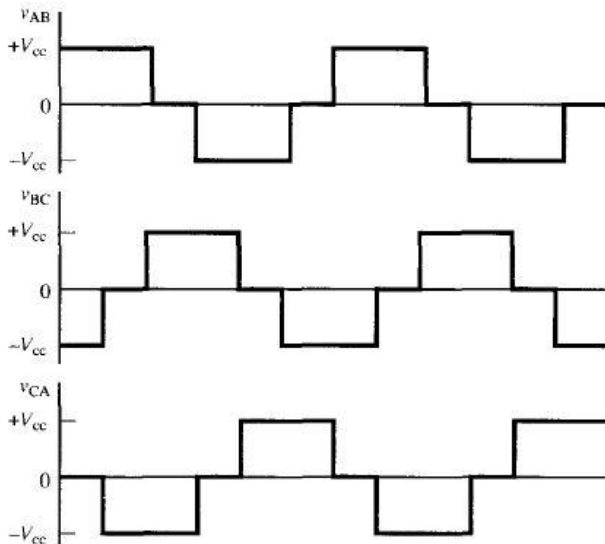


Figure 62. Line-to-line output voltage

As expected results we have first hand that the three phase inverter, designed for the project, fully complies with its purpose since it allows to handle a DC signal and transmit it as AC, Figure 68 and Figure 73, using the pulses, Figure 72, sent from the Mega Arduino in order to generate that the output signals had an offset of 60°, Figure 68.

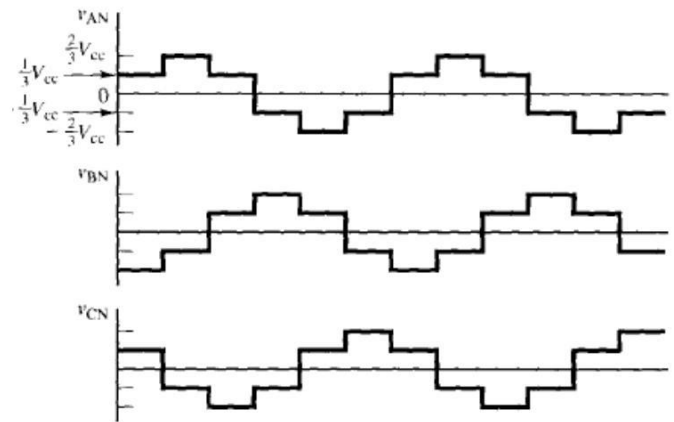


Figure 63. Line-neutral voltage for load connected in star.

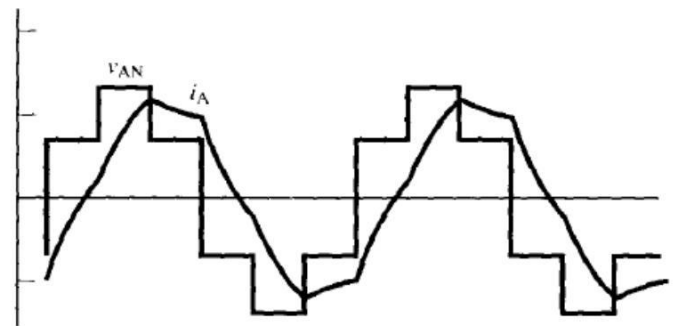


Figure 64. Form of voltage and current output for R-L load.

## VI. RESULTS

The stages of the power control phase are 3, the first stage, orange color Figure 65, allows a virtual coupling of earths to be generated, making this the Mosfet transistors of stage 2, blue color, have their minimum reference in 5V allowing the opening channel of passage to be completely open, consequently making use of the current characteristics of these, which approximately are referenced in maximum in 30th.

Both the first stage, orange color, and the third stage, green color, allow the treatment in phase current of the control signals, Figure 73, sent from the Arduino, so that you have total control over the input and output of the circuit allowing us to condition the external source current to maximum values of 3A per channel without short

circuits, overheating of components or failures in the circuit system in general

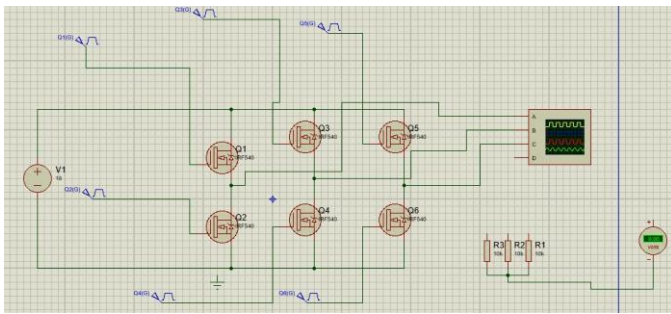


Figure 65. First assembly in Proteus of the three-phase inverter.

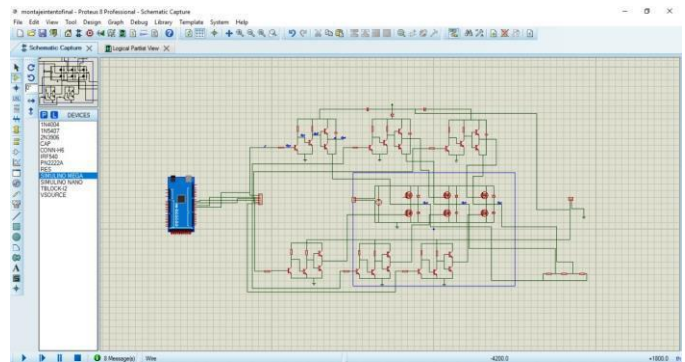


Figure 69. Final stage of circuitry for control of rotation and speed of the axial flux electric motor.

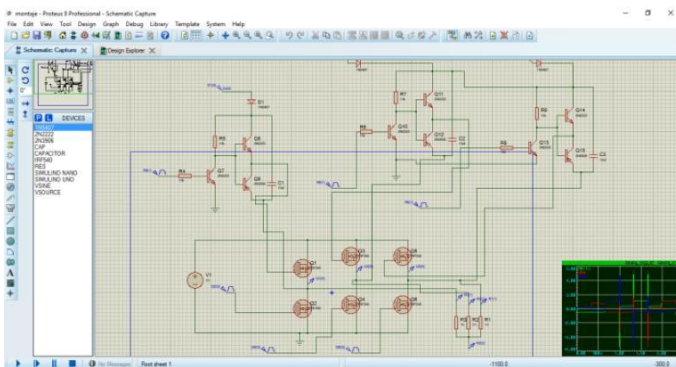


Figure 66. Transistor stage conditioning for current amplification.

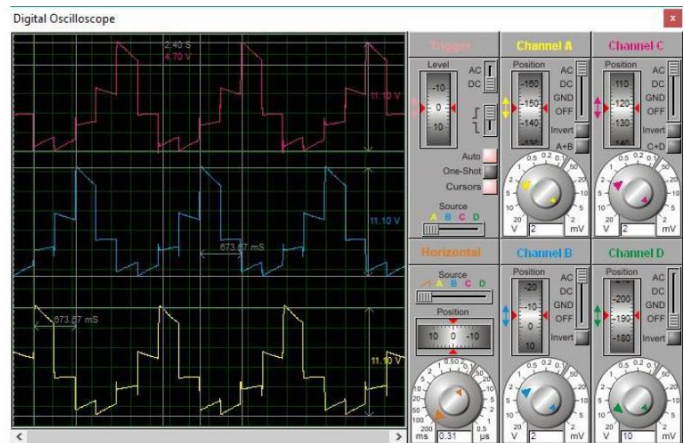


Figure 70. Output of the inverter on each load of the output.

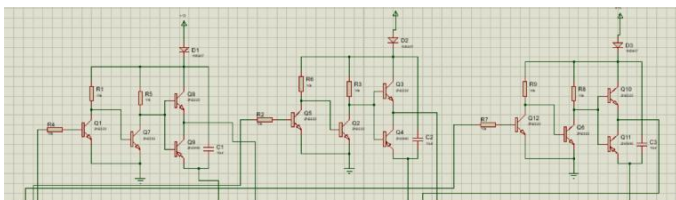


Figure 67. Second stage of current amplification.

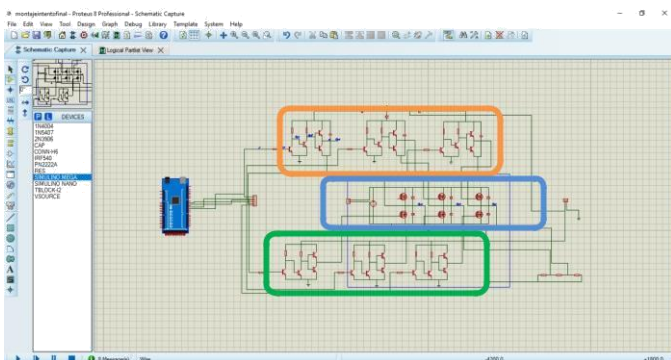


Figure 68. Power control stages.

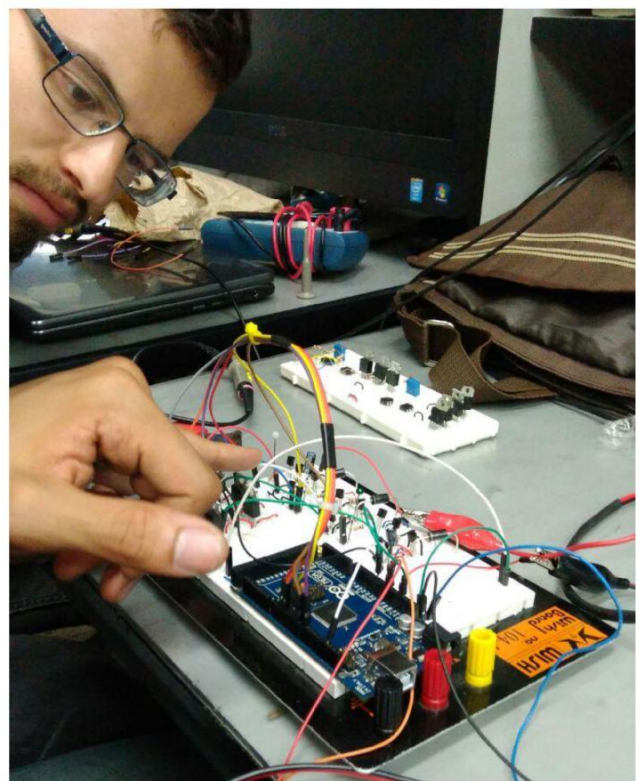


Figure 71. Verification of the assembly for power control.

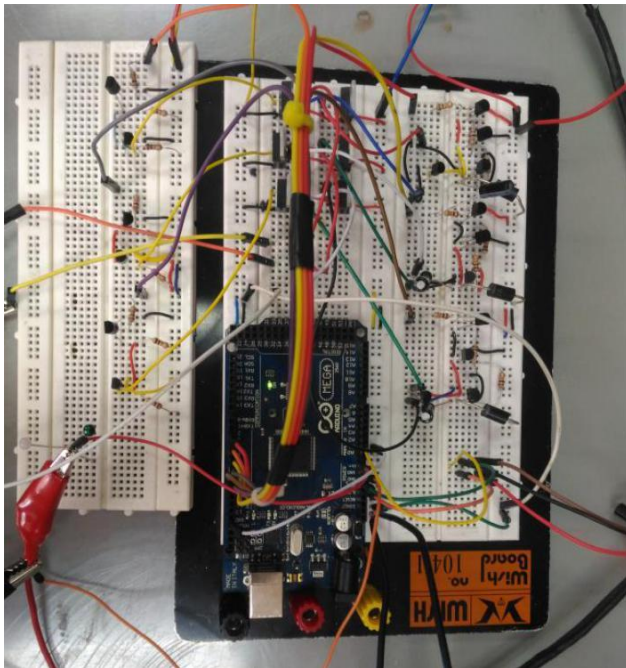


Figure 72. Final assembly for power control.

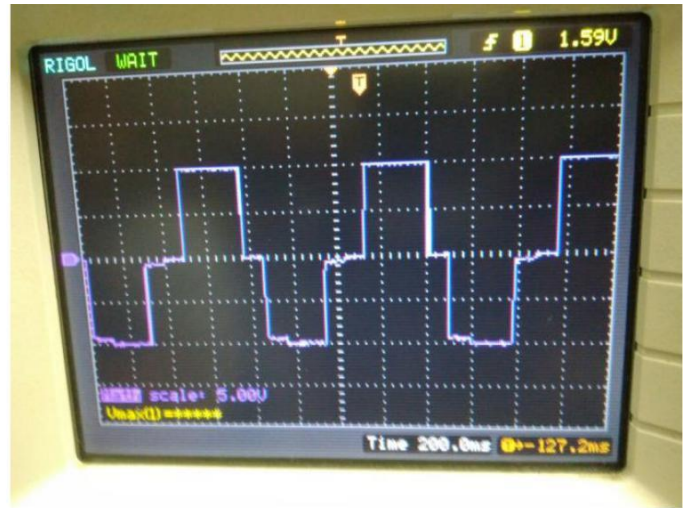


Figure 75. Expected output from the power control stage.

Based on the programs carried out in the Arduino IDE software on the Arduino Mega 2560 embedded system, shown in Figure 77, Figure 78 and Figure 79, the frequency control was performed on the pulses that is necessary to vary the speed with which they present the polarity changes to the coils.

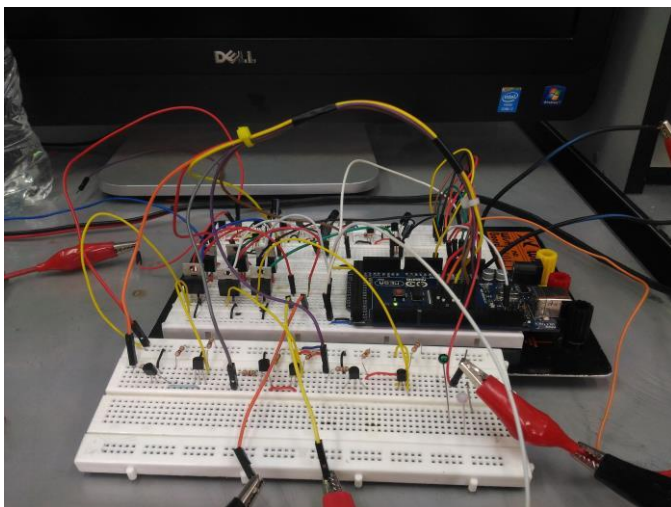


Figure 73. Final assembly test of power control for axial flux electric motor.

```

1 int estado1 = LOW;
2 int estado2 = LOW;
3 int estado3 = LOW;
4 int estado4 = LOW;
5 int estado5 = LOW;
6 int estado6 = LOW;
7 int p1 = 0;
8 int p2 = 0;
9 int p3 = 0;
10 int p4 = 0;
11 int p5 = 0;
12 int p6 = 0;
13
14 void setup() {
15   pinMode(2, OUTPUT);
16   pinMode(3, OUTPUT);
17   pinMode(4, OUTPUT);
18   pinMode(5, OUTPUT);
19   pinMode(6, OUTPUT);
20   pinMode(9, OUTPUT);
21   Serial.begin(9600);
22 }
23
24 void loop() {

```

Figure 76. Program in Arduino Part 1.

```

24 void loop() {
25   float sensorValue = analogRead(A0);
26   // Convert the analog reading (which goes from 0 - 1023) to a voltage (0 - 5V):
27   float voltage = 5 / sensorValue * (10 / 1023.0);
28   // Print out the voltage:
29   Serial.print(" ");
30   //
31   double tau = (1);
32   double te = (tau / 2);
33   float TE = (te * 1000000);
34   float dte = (TE - (0));
35   float dte2 = (TE - (0.33));
36   float dte3 = (TE - (0.66));
37   float dte4 = (TE - (0.99));
38   float dte5 = (TE - (1.32));
39   float dte6 = (TE - (1.65));
40   unsigned long t01 = micros();
41   unsigned long t02 = micros();
42   unsigned long t03 = micros();
43   unsigned long t04 = micros();
44   unsigned long t05 = micros();
45   unsigned long t06 = micros();
46
47   if (t01 - (dte1 + (TE * p1)) >= 0) {

```

Figure 77. Program in Arduino Part 2.

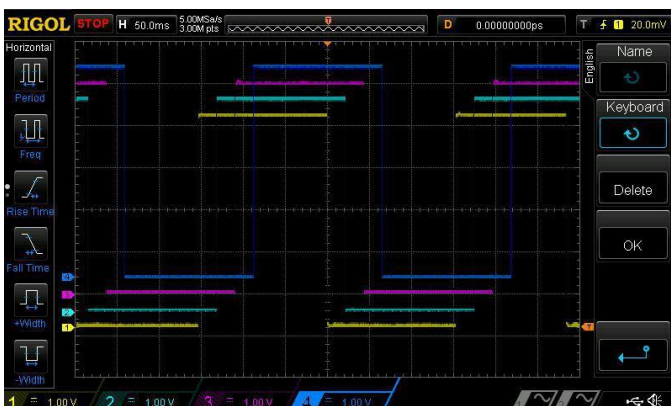


Figure 74. Pulses sent in phase shift.

```

02  estado = 100;
03  }
04  digitalWrite(1, estado);
05  }
06  if (x1 - (45 + (2 * p)) == 0) {
07  p++;
08  if (estado == 100) {
09  estado = 110;
10  } else {
11  estado = 100;
12  }
13  digitalWrite(1, estado);
14  }
15  }
16  if (x1 - (45 + (2 * p)) == 0) {
17  p++;
18  if (estado == 100) {
19  estado = 110;
20  } else {
21  estado = 100;
22  }
23  digitalWrite(1, estado);
24  }
25  }

```

Figure 78. Program in Arduino Part 3.

After carrying out the tests implementing the whole system, it was possible to find the limits of the system, shown in Figure 80 and Figure 81, as minimum and maximum speed, respectively.

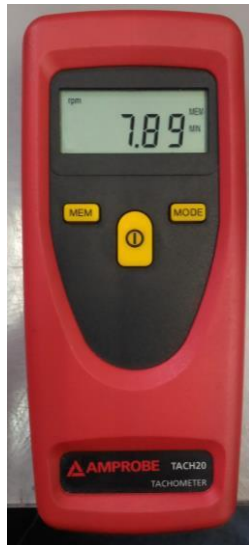


Figure 79. Minimum rpm reached in axial flux electric motor test.



Figure 80. Maximum rpm reached in electric axial flux motor test.

### VII. PHOTOGRAPHIES



Figure 81. Corte laser de acrílico.



Figure 82. Verificación del proceso de corte laser.



Figure 84. Partes para el montaje del motor.



Figure 83. Montaje de magnetssobre el rotor.

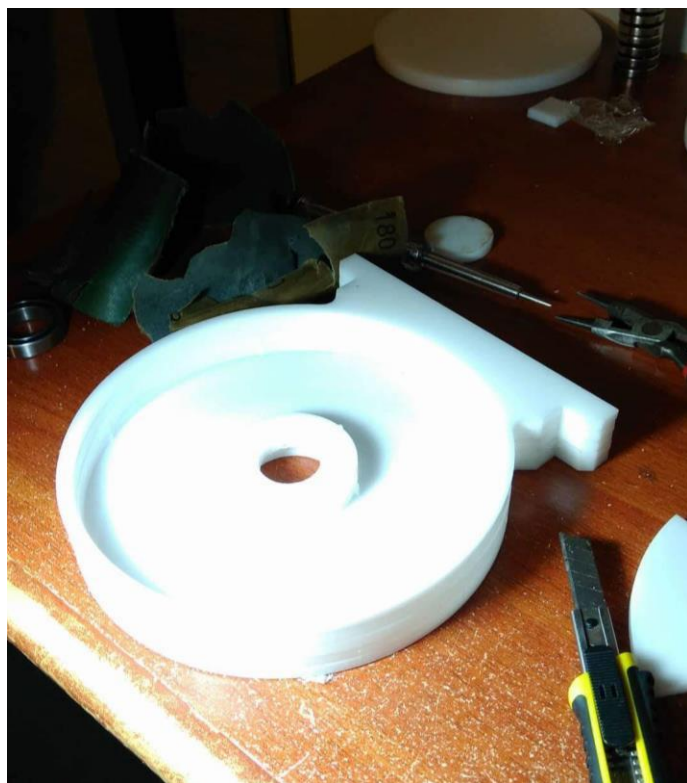


Figure 85. Montaje del estator del motor.



Figure 86. Partes del motor sin ensamblar.



Figure 88. Mecanizado de agujeros para soporte del motor.



Figure 87. Motor de flujo axial ensamblado.

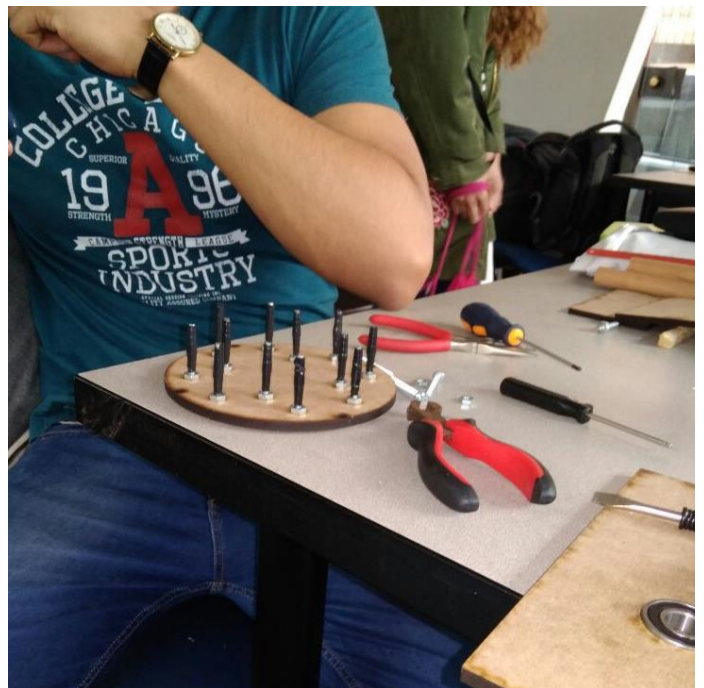


Figure 89. Montaje Molde para Bobinas



Figure 90. Montaje Bobinador

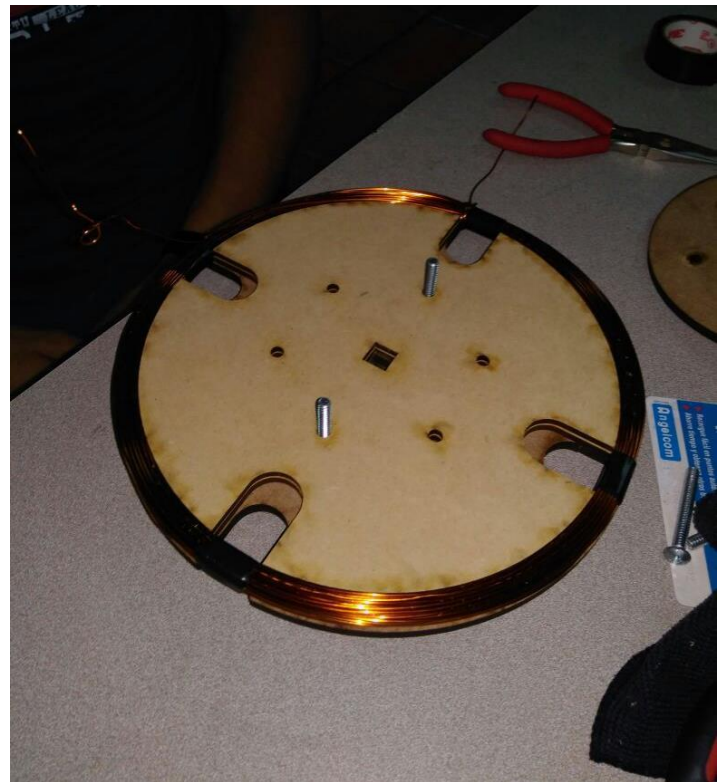


Figure 92. Realización de las bobinas Parte 2.

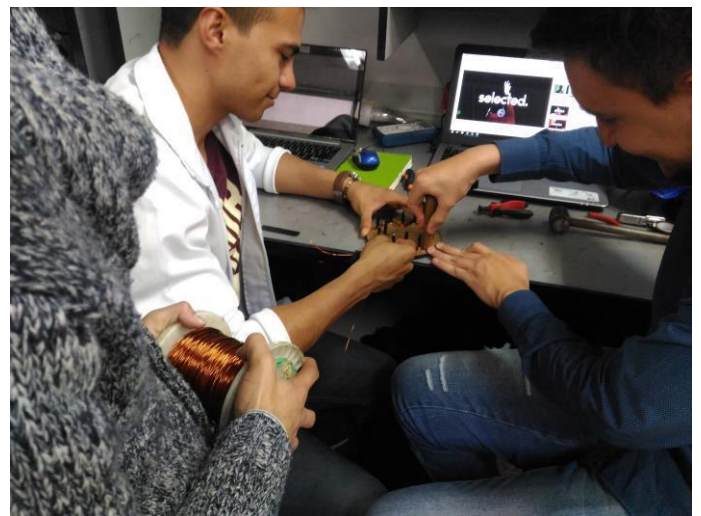


Figure 93. Montaje de las bobinas.



Figure 94. Bobinas modeladas.

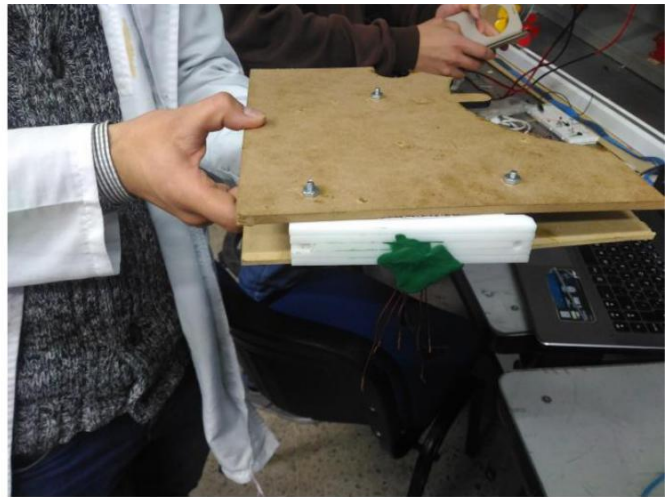


Figure 96. Embebido de bobinas en resina Epoxy.



Figure 97. Bobinas embebidas en resina epoxy.



Figure 95. Grupo de trabajo.



Figure 98. Montaje final del rotor con imanes.

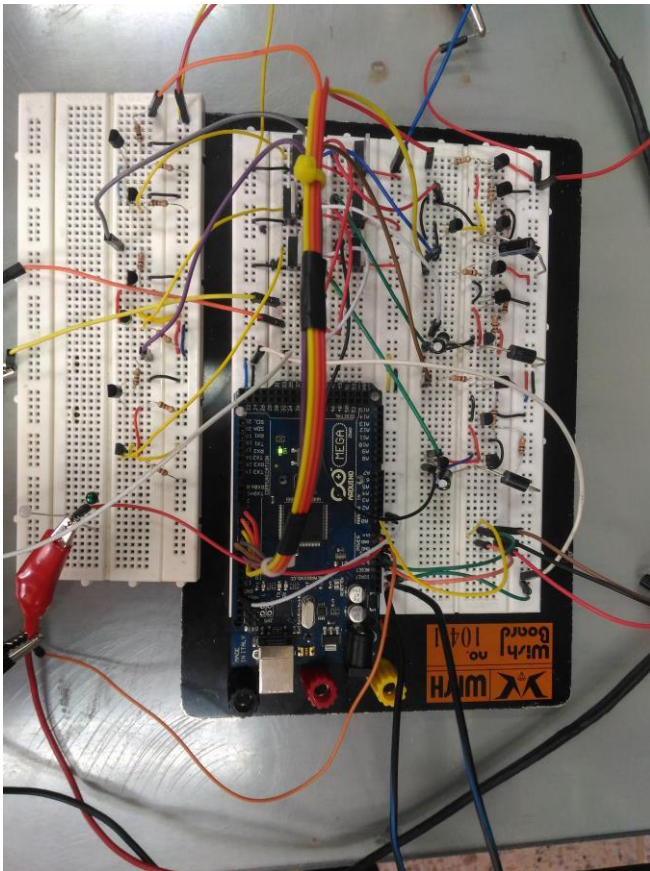


Figure 99. Montaje final de la etapa de control de potencia.

### VIII. CONCLUSIONS

- The geometry of the coil is of great importance since it defines, the level of magnetic field that can be generated, thereby influencing the torque capability.
- The materials chosen for the structure that will serve to support the engine must have strength, flexibility, low weight, low conductivity, in order to reduce the inertia exerted inside the engine as much as possible, the magnetic losses and the generation of parasitic currents induced in the support structure.
- The use of acrylic material for the entire support structure of the engine was supported and defined according to its engineering properties, which allowed us to disregard the variables of weight and magnetic conductivity of the material. In addition, the use of acrylic allowed us to also neglect the inertia and vibrations generated by the movement of the engine at high speeds.
- The use of a three-phase inverter is based on the premise that a DC source is going to be used as an external power source, in order that, in each coil, a sinusoidal power is generated. And so you can, changing the frequency, change the speed of the engine without altering the developed power of it.
- The axial flux electric motor with respect to other conventional motors offers a much higher level of efficiency, torque generation and low presence of vibration due to its geometric topology, distribution of its components affecting the center of mass and its behavior, and mainly that the use of the coils allows mechanical movements to have minimal friction with maximum torque development.
- With the implementation of an axial flux electric motor it is expected to create a path for a better use of the available resources in order to develop a movement towards the optimization of the complete drive system

